

Chemistry of sulfate chloride perhydrates

Part 1.—Thermal decomposition of $4\text{Na}_2\text{SO}_4 \cdot \text{NaCl} \cdot 2\text{H}_2\text{O}_2$ and the formation of $\text{Na}_2\text{SO}_4(\text{III})$

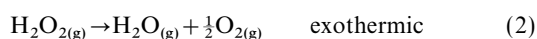
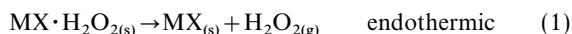
Stephen D. Cosgrove and William Jones

Department of Chemistry, University of Cambridge, Lensfield Road, Cambridge, UK CB2 1EW

Thermal treatment of the perhydrate, $4\text{Na}_2\text{SO}_4 \cdot \text{NaCl} \cdot 2\text{H}_2\text{O}_2$, results in the evolution of H_2O_2 . Combined thermogravimetry (TG) and mass spectrometry (MS) confirms that at least a portion of the H_2O_2 is released intact. TG, together with differential scanning calorimetry (DSC), suggests that the release of H_2O_2 occurs in two stages. The isothermal decomposition of the perhydrate at 88°C has been monitored by powder X-ray diffraction (PXRD), IR spectroscopy, available oxygen content (AVOX) and thermogravimetry. The resulting solid consists of an intimate mixture of $\text{Na}_2\text{SO}_4(\text{III})$ and NaCl. An explanation for the formation of this particular polymorphic form of Na_2SO_4 is proposed.

Perhydrates, compounds containing hydrogen peroxide of crystallisation, are important components of powder laundry detergents. The crystal structures of several perhydrates have been determined including adducts with urea,¹ Na_2CO_3 ,² KF ,³ $\text{M}_2\text{C}_2\text{O}_4$ ($\text{M} = \text{Li}$,⁴ Na ,⁵ K ,⁶ Rb ,⁷ NH_4)⁸ and guanidinium salts.⁹ Of interest is the relatively stable perhydrate, $4\text{Na}_2\text{SO}_4 \cdot \text{NaCl} \cdot 2\text{H}_2\text{O}_2$ (SSCP), developed for use with neutral detergents.¹⁰ Structural analysis of SSCP has shown that the H_2O_2 is included within channels defined by sulfate oxygens in the *ab* plane.¹¹

The DSC traces of perhydrates have been found to give a mixture of endothermic and exothermic events because two reactions are occurring.¹² The first reaction, eqn. (1), is endothermic deperhydration (*i.e.* release of H_2O_2), whilst the second is the exothermic decomposition of gaseous H_2O_2 in the vicinity of the sensors [eqn. (2)].



If the perhydrate decomposes at a temperature sufficiently low to prevent rapid decomposition of the H_2O_2 , then only an endotherm is observed (*e.g.* $\text{Na}_2\text{C}_2\text{O}_4 \cdot \text{H}_2\text{O}_2$).¹² At higher temperatures decomposition of the H_2O_2 can render the reaction exothermic (*e.g.* $\text{K}_2\text{C}_2\text{O}_4 \cdot \text{H}_2\text{O}_2$).¹² However, the DSC traces are usually not this simple and a number of exotherms are often superimposed onto the endotherm [*e.g.* $[\text{C}(\text{NH}_2)_3]_4 \cdot \text{P}_2\text{O}_7 \cdot 1.5\text{H}_2\text{O} \cdot \text{H}_2\text{O}_2$].¹³

The isothermal decomposition of $\text{Na}_2\text{CO}_3 \cdot 1.5\text{H}_2\text{O}_2$ ^{14,15} and of the oxalate perhydrates¹² have been reported. Comparison of α/t vs. t plots with theoretical curves¹⁶ are able to give an indication of obedience to particular kinetic laws, where α is the extent of reaction. These perhydrates exhibit examples of kinetic behaviour described by Avrami–Erofeev [$-\ln(1-\alpha) = kt^n$], power law ($\alpha = kt^n$) and contracting solid [*e.g.* $1 - (1-\alpha)^{1/2} = kt$] models.^{12,14}

We have previously reported that the thermal decomposition of SSCP does not result in a simple mixture of Na_2SO_4 and NaCl (using laboratory grade reagents for comparison).¹⁷ Na_2SO_4 , however, has five polymorphic forms.¹⁸ Standard laboratory grade Na_2SO_4 is predominantly the room temperature phase (V). The other polymorphs of Na_2SO_4 are formed when phase V is heated. $\text{Na}_2\text{SO}_4(\text{III})$ is formed at 238°C .¹⁸ Phases II and I form at higher temperatures and revert to phase III on cooling. Once formed, $\text{Na}_2\text{SO}_4(\text{III})$ remains stable in dry air almost indefinitely¹⁹ but water causes rapid transformation to $\text{Na}_2\text{SO}_4(\text{V})$.²⁰

SSCP represents one of the few purely inorganic inclusion compounds not composed of Si–O or Al–O units, or transition metals. We are also unaware of any other inorganic inclusion compounds containing H_2O_2 as the guest species. In this paper we discuss in detail the nature of the thermal decomposition of SSCP and show that the high temperature phase (III) of Na_2SO_4 is formed along with NaCl after H_2O_2 evolution.

Experimental

Using laboratory grade reagents, a solution of 0.42 g ($7.2 \times 10^{-3}\text{ mol}$) NaCl in 8 g of 0.30 g cm^{-3} H_2O_2 was added dropwise to a solution of 4.09 g ($28.8 \times 10^{-3}\text{ mol}$) of Na_2SO_4 in 20 g of 0.30 g cm^{-3} H_2O_2 . The resulting solution was allowed to evaporate in air and yielded well formed crystals of SSCP. These were ground (grinding did not affect the structure or H_2O_2 content) and the powder dispersed in Petri dishes. These samples were placed in a preheated isothermal Gallenkamp oven and removed periodically and immediately refrigerated at 0°C in order to prevent further decomposition. Analyses (PXRD, TG, IR) were then performed at ambient temperature as soon as possible. In particular, AVOX measurements were recorded to determine the oxygen content available for oxidation: a solution of *ca.* 0.2 g of SSCP in 100 cm^3 of 10% H_2SO_4 was titrated against a 0.1 M solution of potassium permanganate. Evidence for obedience to a particular kinetic law can be obtained from α/t vs. t plots using eqn. (3):

$$\alpha = (A_0 - A)/A_0 \quad (3)$$

where A_0 is the initial AVOX value and A is the AVOX at time t .

TG data on ground SSCP were collected using a heating rate of $10^\circ\text{C min}^{-1}$, and a N_2 flow of $25\text{ cm}^3\text{ min}^{-1}$. Combined TG–MS was performed using a heating rate of $30^\circ\text{C min}^{-1}$. Full details of the apparatus have been described elsewhere.²¹ DSC was performed on a Perkin–Elmer 7-series instrument, with an argon gas flow of $30\text{ cm}^3\text{ min}^{-1}$ and a heating rate of $10^\circ\text{C min}^{-1}$.

²³Na NMR spectra were recorded on a Chemagnetics CMX-400 spectrometer at 105.8 MHz (9.4 T) with 4 mm probe head. Magic angle spinning (MAS) Bloch delay measurements were recorded at a spinning rate of 10 kHz with 0.3 ms short pulses ($<15^\circ$) and 2 ms (90°) pulses. The short pulse measurements give the quantitative intensity ratio of Na sites with different quadrupole interactions, whereas the 90° pulse measurements preliminarily detect Na sites with different quad-

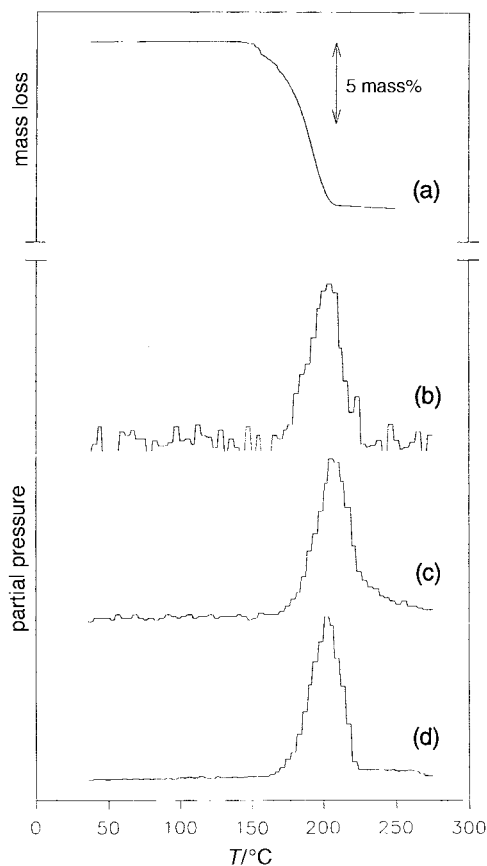


Fig. 1 TG-MS traces of SSCP: (a) TG; MS scanning; (b) m/z 34 (H_2O_2); (c) m/z 18 (H_2O); (d) m/z 32 (O_2)

rupole interaction since the relative intensity of Na site with large quadrupole interaction decreases in comparison with that in the short pulse spectrum. The ^{23}Na chemical shifts are given in ppm from an external 1 M NaCl aqueous solution.

Results

Thermal analysis

Fig. 1(a) shows the thermogravimetric curve of SSCP. Fig. 1(b), (c) and (d) indicate the mass signal as a function of temperature for m/z 34 (H_2O_2), m/z 18 (H_2O) and m/z 32 (O_2). The TG curve shows a single distinct mass loss of 9.8% between 150 and 200 °C, corresponding to the loss of two H_2O_2 per formula unit (expected 9.8%). Peaks in the mass signal are observed coincident with this mass loss.

Fig. 2(a) shows the DSC trace for SSCP. A broad endotherm coincides with the TG mass loss (150–200 °C) and corresponds to deperhydration [eqn. (1)]. The endotherm is immediately followed by an exotherm at ca. 200 °C. This exotherm does not coincide with any mass loss and is associated with the decomposition of evolved H_2O_2 within the vicinity of the sensors [eqn. (2)].¹² A small exothermic event is also measured at 190 °C (peak 2). The DTG curve is displayed in Fig. 2(b). The single mass loss in the TG [Fig. 1(a)] is resolved into two DTG peaks (3,4). The temperature at which the rate of evolution of H_2O_2 increases (3) coincides with the start of the first exotherm (1). The minimum of the main DTG peak (4) corresponds to the centre of that exotherm (2). It therefore seems likely that an exothermic event occurs during which the release of H_2O_2 is facilitated.

Isothermal decomposition of SSCP at 88 °C

Some perhydrates decompose to give a hydrate intermediate. In humid conditions at room temperature, the oxalate

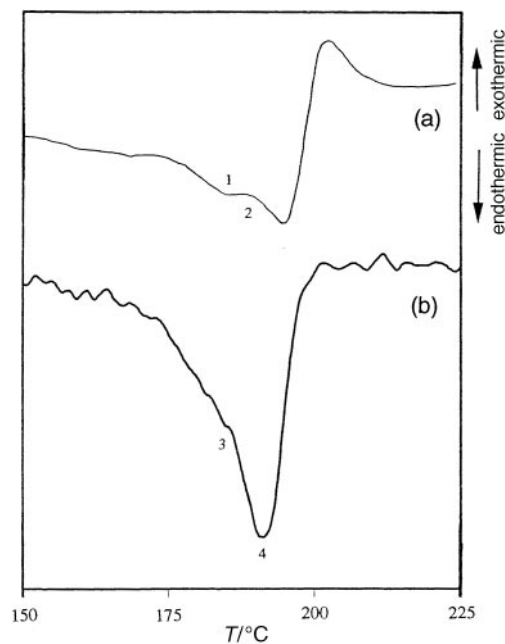


Fig. 2 (a) DSC and (b) DTG of SSCP

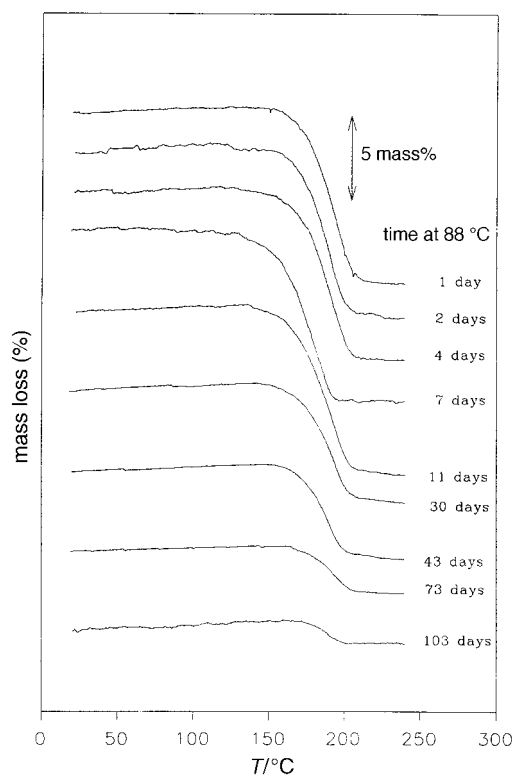


Fig. 3 TG traces of samples of SSCP after heating at 88 °C

$\text{K}_2\text{C}_2\text{O}_4 \cdot \text{H}_2\text{O}_2$ decomposes to give $\text{K}_2\text{C}_2\text{O}_4 \cdot \text{H}_2\text{O}$.²² There is also evidence that the thermal decomposition of $\text{Na}_2\text{CO}_3 \cdot 1.5\text{H}_2\text{O}_2$ results in a hydrate.²³ We were interested to discover whether a hydrate such as $4\text{Na}_2\text{SO}_4 \cdot \text{NaCl} \cdot 2\text{H}_2\text{O}$ formed from SSCP at temperatures below 100 °C.

Fig. 3 shows TG curves for samples of SSCP which have been previously held at 88 °C for up to 103 days. Each curve shows a mass loss occurring typically in the range 150–200 °C. There is no evidence for any mass loss below 150 °C, which would be indicative of an intermediate hydrate. AVOX measurements show that after more than 100 days at 88 °C, there is still some residual H_2O_2 within the sample. Fig. 4 shows the α/t vs. t plot for the deperhydration of SSCP at

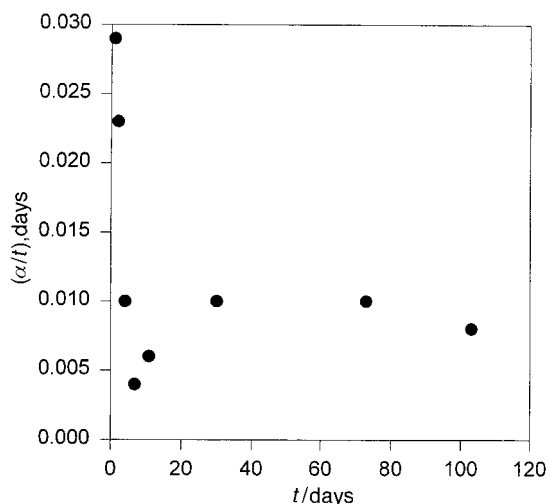


Fig. 4 α/t vs. t plot of samples of SSCP after heating at 88 °C

88 °C, using eqn. (3). Comparing the shape of the curve to those described by Guarini and Spinicci,¹⁶ the initial drop in α/t may correspond to obedience to the contracting circle model. Beyond 10 days α/t appears to rise and then fall, suggesting Avrami–Erofeev ($n=2$) obedience.

Powder X-ray diffraction patterns monitoring the deperhydration of SSCP at 88 °C are shown in Fig. 5. The patterns show a gradual change from SSCP to Na₂SO₄ (either phase III or phase V) in agreement with AVOX–time plots. All the reflections in Fig. 5 can be assigned as SSCP, Na₂SO₄ or NaCl. Fig. 6 shows the variation in intensity of the (202) reflection of SSCP at 27.1°, the Na₂SO₄(III) (111) reflection at 22.6°, and the Na₂SO₄(V) (131) reflection at 28.1°. The SSCP reflection shows an initial increase in intensity followed by a gradual decrease from 30 days. The Na₂SO₄(V) reflection at 28.1° rises and then falls. This fall mirrors the rise in the Na₂SO₄(III) reflection at 22.6°.

Isothermal decomposition of SSCP at 126 and 183 °C show similar trends in the PXRD to that at 88 °C.

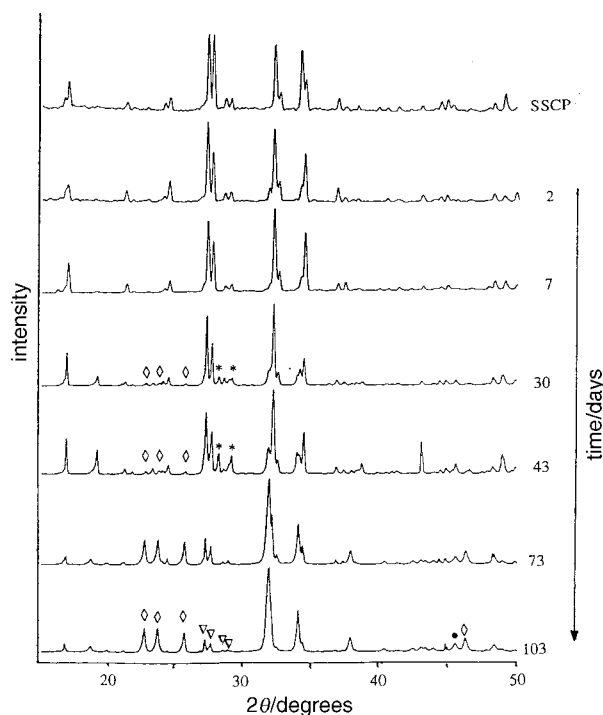


Fig. 5 PXRD patterns of samples of SSCP after heating at 88 °C (▽, SSCP; ◇, Na₂SO₄(III); *, Na₂SO₄(V); ●, NaCl. For clarity, only representative reflections are labelled)

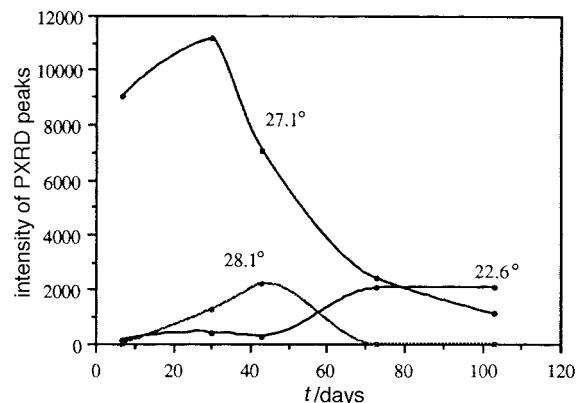


Fig. 6 Changes in intensities of PXRD reflections at 22.6, 27.1 and 28.1° in samples of SSCP heated at 88 °C

Characterisation of the product of thermal deperhydration of SSCP

The solid resulting from the thermal decomposition of SSCP when all the H₂O₂ has evolved is denoted SSCPD. Fig. 7 compares the experimental PXRD pattern of SSCPD with simulated patterns of Na₂SO₄(III) and NaCl [using the crystal structures of Na₂SO₄(III)²⁴ and NaCl²⁵ and the molecular modelling package CERIUS²].²⁶ It is apparent that the host lattice of SSCP does not remain intact but breaks down into Na₂SO₄(III) and NaCl.

The formation of Na₂SO₄(III) when all the H₂O₂ is thermally removed from SSCP is also indicated by ²³Na 90° pulse solid state NMR (Fig. 8) in that two sharp peaks are observed for SSCPD. Samples of pure Na₂SO₄(V) gave an identical trace to a ground physical mixture of NaCl + 4Na₂SO₄(V), only without the NaCl peak at δ 7.

Na₂SO₄(V) has a complex set of peaks upfield (Fig. 8) corresponding to the distorted coordination present. Nord showed there is just one Na crystallographic site in Na₂SO₄(V), coordinated by six oxygens.²⁷ These NaO₆ octahedra are very distorted (O···Na···O angles ranging from 56.1 to 134.8°). Conversely, Mehrotra showed that Na₂SO₄(III) has two distinct Na atoms present in the unit cell.²⁴ This difference is reflected in the solid state NMR spectrum. There is a large single peak at δ -2, corresponding to the nearly regular Na(2)

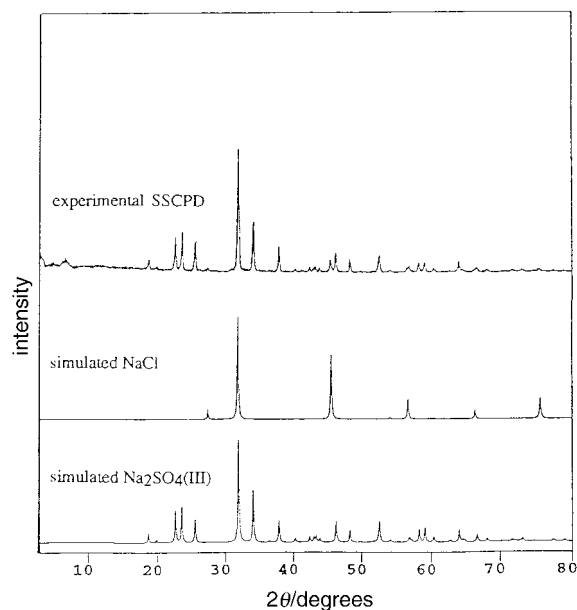


Fig. 7 Experimental PXRD pattern of SSCP compared to simulated PXRD patterns of Na₂SO₄(III) and NaCl

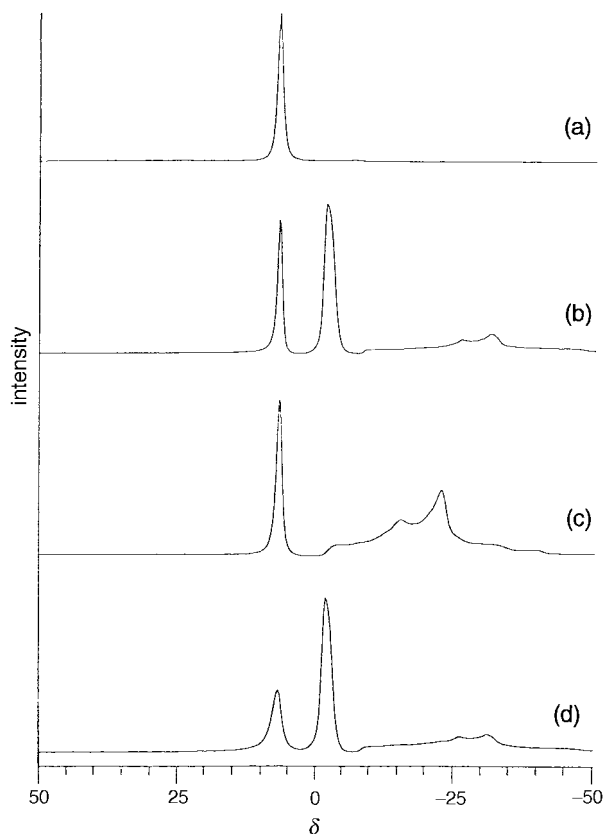


Fig. 8 Solid state ^{23}Na NMR spectra of (a) NaCl, (b) 4:1 $\text{Na}_2\text{SO}_4(\text{III})$ and NaCl, (c) 4:1 $\text{Na}_2\text{SO}_4(\text{V})$ and NaCl and (d) SSCPD

Table 1 Comparison of IR bands measured for SSCPD, $\text{Na}_2\text{SO}_4(\text{V})$ and $\text{Na}_2\text{SO}_4(\text{III})^a$

SSCPD/ cm^{-1}	$\text{Na}_2\text{SO}_4(\text{III})/\text{cm}^{-1}$	$\text{Na}_2\text{SO}_4(\text{V})/\text{cm}^{-1}$	SO_4 assignment
1137s (br)	1142s (br)	—	ν_3
—	—	1127s (br)	ν_3
1104s (br)	1106s (br)	—	ν_3
995(sh)	995(sh)	—	ν_1
635s	635s	637s	ν_4
623s	622s	—	ν_4
614s	614s	615s	ν_4

^as = strong, br = broad, sh = shoulder.

octahedral environment ($\text{O}\cdots\text{O}$ angles ranging from 82.9 to 97.1°). The more complex peaks upfield are identified with the less symmetrical $\text{Na}(1)$ ($\text{O}\cdots\text{Na}\cdots\text{O}$ angles ranging from 58.1 to 116.2°). The environments of the Na ions in SSCPD are clearly similar to those in a $4\text{Na}_2\text{SO}_4(\text{III})/\text{NaCl}$ mixture. The differences in signal width and intensity of the NaCl peak at $\delta 7$ probably arise from factors such as particle size and the far greater dispersion of NaCl amongst Na_2SO_4 particles in SSCPD.

Table 1 compares the bands observed in the IR spectrum of SSCPD to those of $\text{Na}_2\text{SO}_4(\text{III})$ and $\text{Na}_2\text{SO}_4(\text{V})$. All IR bands measured for SSCPD are coincident with all the bands measured for $\text{Na}_2\text{SO}_4(\text{III})$. In particular, SSCPD shows a strong broad doublet at $1104/1137\text{cm}^{-1}$ and a sharp band at 995cm^{-1} . The latter band is absent in the spectrum for $\text{Na}_2\text{SO}_4(\text{V})$ since the ν_1 mode is forbidden and only a strong broad singlet is observed at 1127cm^{-1} .

Discussion

Thermal analysis

The TG–MS trace scanning $m/z 34$ reveals that at least some H_2O_2 is released intact when SSCPD is heated. Indeed this is in

accord with the observation that SSCPD deperhydrates to form $\text{Na}_2\text{SO}_4(\text{III})$ rather than $\text{Na}_2\text{SO}_4(\text{V})$: since water catalyses the $\text{III}\rightarrow\text{V}$ transformation, this implies an absence of H_2O during deperhydration and thus release of intact H_2O_2 . It is therefore probable that the presence of a peak at $m/z 18$, is due to decomposition of H_2O_2 en route to the mass spectrometer. The release of intact H_2O_2 has also been reported for the thermal decomposition of guanidinium salt perhydrates¹³ and of oxalate perhydrates.¹²

The existence of two DTG peaks suggests there are two phases of H_2O_2 evolution, of which the second is the more rapid. The formation of cracks would facilitate the removal of H_2O_2 by increasing the surface area. Cracking has been observed for the thermal decomposition of SSCPD by hot stage optical microscopy and SEM.²⁸ Fig. 2 suggests that upon heating SSCPD, H_2O_2 close to the surface is released first leaving a barrier product layer of $\text{Na}_2\text{SO}_4(\text{III})$ and NaCl. Formation of a barrier product layer has been reported for $\text{Na}_2\text{CO}_3\cdot 1.5\text{H}_2\text{O}_2$.¹⁴ H_2O_2 which is more deeply buried into the crystallite cannot, however, permeate this barrier product layer. Continued heating results in cracking, thus increasing the surface area. The increase in surface area and the higher temperature enables rapid release of the residual H_2O_2 . The decomposition of any initial release of H_2O_2 (from near the surface of the crystallite) may also contribute to the exothermic event at 190°C .

Isothermal treatment

The thermal behaviour of SSCPD, as monitored by PXRD, is similar at 88 to that at 126°C .¹⁷ At both temperatures, changes in the PXRD are more-or-less gradual. This implies that the SSCPD host is unstable in the absence of guest H_2O_2 molecules and that loss of H_2O_2 is accompanied by immediate phase separation into $\text{Na}_2\text{SO}_4(\text{III})$ and NaCl.

There is no evidence in the TG traces for formation of an intermediate hydrate during thermal deperhydration since no mass loss is observed below 150°C . All the reflections in the PXRDs have been assigned as either SSCPD, $\text{Na}_2\text{SO}_4(\text{III})$, $\text{Na}_2\text{SO}_4(\text{V})$ or NaCl, also indicating that hydrate formation does not occur.

AVOX values evidencing deperhydration of SSCPD, appear to best fit the contracting solid kinetic model up to 10 days heating at 88°C . The kinetic behaviour then changes from contracting solid to Avrami–Erofeev ($n=2$). This behaviour is in contrast to that observed for SSCPD at 126°C for which the contracting solid model is obeyed throughout.²⁸ The assignments of rate laws to the thermal deperhydration of SSCPD are made tentatively since the α/t vs. t plot is ambiguous.¹⁶

Product of deperhydration

Upon heating SSCPD, the inclusion host does not remain intact. Neither does it form the usual phase V polymorph of Na_2SO_4 . Instead NMR, PXRD and IR evidence that $\text{Na}_2\text{SO}_4(\text{III})$ and NaCl are formed. Although $\text{Na}_2\text{SO}_4(\text{III})$ is stable at room temperature in the absence of moisture, it is normally regarded as a high temperature phase of Na_2SO_4 . The reason for the stability of $\text{Na}_2\text{SO}_4(\text{III})$ at room temperature is not apparent in the literature concerning Na_2SO_4 . Buerger noted, however, that ‘if the temperature is varied beyond the stability range of a structure, and the failure of a sluggish transformation prevents the change of structure to the stable form (phase V), the phase may be said to be stranded.’²⁹ $\text{Na}_2\text{SO}_4(\text{III})$ may be regarded as an example of a stranded phase.

$\text{Na}_2\text{SO}_4(\text{III})$ and NaCl are formed at 88 , 126 and 183°C . It is possible that $\text{Na}_2\text{SO}_4(\text{III})$ is preferentially formed at even lower temperatures than 88°C . As the temperature is lowered to below 100°C , however, the water catalysed $\text{III}\rightarrow\text{V}$ transformation may become more active. Thus deperhydration at say 60°C , though initially forming $\text{Na}_2\text{SO}_4(\text{III})$ and NaCl,

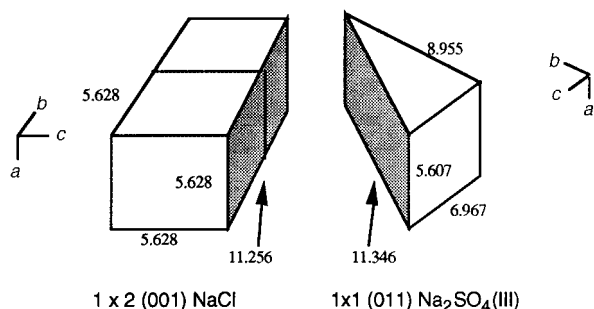


Fig. 9 Epitaxial relationship between $\text{Na}_2\text{SO}_4(\text{III})$ and NaCl . The shaded faces have areas within 1% of each other (distances in Å).

may result in a mixture of $\text{Na}_2\text{SO}_4(\text{III})$ and (V) phases. This process may be indicated by the PXRD of SSCP after 43 days heating at 88°C , in which some $\text{Na}_2\text{SO}_4(\text{V})$ is visible (Fig. 5 and 6). Deperhydration studies at 60°C would, however, be impractical owing to the high stability of SSCP.

We propose that the preferential formation of $\text{Na}_2\text{SO}_4(\text{III})$ over $\text{Na}_2\text{SO}_4(\text{V})$ is due to the existence of epitaxial relationships between the unit cell dimensions of $\text{Na}_2\text{SO}_4(\text{III})$ and NaCl and between those of NaCl and SSCP. In epitaxy the crystals of one phase (guest crystals) grow on the surface of a crystal of another phase (host crystal) in one or more strictly defined crystallographic orientations.³⁰ Epitaxial growth requires that the interface between the two crystals be of similar surface area and shape, and results in an enhanced rate of formation. Fig. 9 reveals that the dimensions of the 1×1 (011) face of the $\text{Na}_2\text{SO}_4(\text{III})$ crystal are within 1% of those of the 2×1 (001) face of the NaCl crystal. In the same way the dimensions of the 1×1 (112) face of the SSCP crystal are within 1% of those of the 2×2 (001) face of the NaCl crystal. Faces with such similar surface areas to those of NaCl and SSCP could not be found for $\text{Na}_2\text{SO}_4(\text{V})$ (unit cell: 5.86, 12.304, 9.817 Å). The $\text{Na}_2\text{SO}_4(\text{III})$ phase is therefore able to preferentially form by growing on the surface of NaCl crystals which are formed during decomposition.

Conclusions

The unusually stable perhydrate $4\text{Na}_2\text{SO}_4 \cdot \text{NaCl} \cdot 2\text{H}_2\text{O}_2$ (SSCP) has been shown to give $\text{Na}_2\text{SO}_4(\text{III})$ and NaCl upon thermal decomposition. At least some of the H_2O_2 is released intact. At 88°C decomposition behaviour appears first to follow contracting solid kinetics and subsequently those described by the Avrami–Erofeev ($n=2$) equation. Decomposition of SSCP results in the formation of $\text{Na}_2\text{SO}_4(\text{III})$ rather than $\text{Na}_2\text{SO}_4(\text{V})$ owing to epitaxial growth on the surface of the crystallites. We demonstrate in Part 2³¹ of this series that the perhydrate can be regenerated by exposing SSCPD to the vapour above a H_2O_2 solution.

The financial assistance of EPSRC and Solvay Interlox Ltd. (CASE award to S. D. C.) is appreciated. We also thank Drs J. Klinowski and H. He for performing solid state NMR spectroscopy and Dr J. P. Attfield for helpful discussions.

References

- 1 C. J. Fritchie Jr. and R. K. McMullan, *Acta Crystallogr., Sect. B*, 1981, **37**, 1086.
- 2 J. M. Adams, R. G. Pritchard and A. W. Hewat, *Acta Crystallogr., Sect. B*, 1979, **35**, 1759.
- 3 V. A. Sarin, V. Ya. Dudarev, T. A. Dobrynina, L. E. Fykin and V. E. Zavadnik, *Sov. Phys. Crystallogr.*, 1976, **21**, 531.
- 4 B. F. Pedersen, *Acta Chem. Scand.*, 1969, **23**, 1871.
- 5 B. F. Pedersen and A. Kvik, *Acta Crystallogr., Sect. C*, 1989, **45**, 1724.
- 6 B. F. Pedersen and A. Kvik, *Acta Crystallogr., Sect. C*, 1990, **46**, 21.
- 7 B. F. Pedersen, *Acta Chem. Scand.*, 1967, **21**, 779.
- 8 B. F. Pedersen, *Acta Crystallogr., Sect. B*, 1972, **28**, 746.
- 9 J. M. Adams and R. G. Pritchard, *Acta Crystallogr., Sect. B*, 1976, **32**, 2438; J. M. Adams and V. Ramdas, *Acta Crystallogr., Sect. B*, 1978, **34**, 2150; 2781; *Inorg. Chim. Acta*, 1979, **34**, L225.
- 10 Kao Soap Co. Ltd. and Nippon Peroxide Co. Ltd., *Ger. Pat.*, 2530 539, 1975.
- 11 J. M. Adams and V. Ramdas, *Acta Crystallogr., Sect. B*, 1981, **37**, 915.
- 12 J. M. Adams, V. Ramdas, G. G. T. Guarini and C. J. Adams, *J. Chem. Soc., Dalton Trans.*, 1980, 269.
- 13 C. J. Adams, J. M. Adams, R. G. Pritchard and V. Ramdas, *J. Inorg. Nucl. Chem.*, 1979, **41**, 937.
- 14 A. K. Galwey and W. J. Hood, *J. Phys. Chem.*, 1979, 1810.
- 15 A. K. Galwey and W. J. Hood, *J. Chem. Soc., Faraday Trans. 1*, 1982, **78**, 2815.
- 16 G. G. T. Guarini and R. Spinicci, *J. Therm. Anal.*, 1972, **4**, 435.
- 17 S. D. Cosgrove and W. Jones, *J. Chem. Soc., Chem. Commun.*, 1994, 2255.
- 18 B. N. Mehrotra, *Phase Transitions*, 1989, **16/17**, 431.
- 19 G. E. Brodale and W. F. Giaque, *J. Phys. Chem.*, 1972, **76**, 737.
- 20 M. Sakaguchi, M. Ohta and S. Miyazaki, *J. Electrochem. Soc.*, 1984, **131**, 1942.
- 21 I. C. Chisem, S. D. Cosgrove and W. Jones, *J. Therm. Anal.*, in press.
- 22 J. M. Adams, L. A. Ashe and C. J. Adams, *Inorg. Chim. Acta*, 1980, **44**, L195.
- 23 Solvay Interlox Ltd., personal communication.
- 24 B. N. Mehrotra, *Z. Kristallogr.*, 1981, **155**, 159.
- 25 R. W. G. Wyckoff, *The Structure of Crystals*, ACS Monograph Series, 1931, p. 227, 1995.
- 26 CERIU² version 2.0, BIOSYM/MSI Inc., The Quorum, Cambridge, UK.
- 27 A. G. Nord, *Acta Chem. Scand.*, 1973, **27**, 814.
- 28 S. D. Cosgrove, PhD Thesis, University of Cambridge, 1996.
- 29 M. J. Buerger, in *Phase Transformations in Solids*, ed. R. Smoluchowski, J. E. Mayer and W. A. Weyl, Wiley, New York, 1951, pp. 183–199.
- 30 I. Bonev, *Acta Crystallogr., Sect. A*, 1972, **28**, 508.
- 31 S. D. Cosgrove and W. Jones, *J. Mater. Chem.*, following paper.

Paper 7/06384I; Received 1st September, 1997